DOI: 10.1002/chem.200601126

The Supramolecular Helical Architecture of 8-Oxoinosine and 8-Oxoguanosine Derivatives

Stefano Lena,[a] Mauro A. Cremonini,[b] Francesco Federiconi,[c] Giovanni Gottarelli,*[a] Carla Graziano,[a] Luca Laghi,[b] Paolo Mariani,[c] Stefano Masiero,[a] Silvia Pieraccini,[a] and Gian Piero Spada*[a]

Abstract: The 8-oxoguanosine derivative **1** and the 8-oxoinosine derivative **2b**, with appropriate substituents on their ribose moieties, form hexagonal lyotropic mesophases in hydrocarbon solvents. Small-angle X-ray scattering analysis of a film of **1** and of the mesophase of **2b**, and NMR and CD spectra of isotropic solutions of **2b**, indicate that in both cases the supramolecular structures adopted are continuous helices formed by a hydrogen-bond network between the heterocyclic bases. Notably, while derivative **2b**, which bears large substituents on its ribose moiety, undergoes self-assembly and mesophase formation, oxoinosine **2a**, with only decanoyl groups on its ribose moiety, does not. This may be ascribed to the reduced amphiphilic properties of the latter and the absence of aromatic groups.

Keywords: liquid crystals · oxoguanosine · oxoinosine · self-assembly · supramolecular chemistry

Introduction

The construction of complex structures based on weak interactions is one of the major goals of supramolecular chemistry;[1] on the other hand, helical structures occur widely in Nature and are responsible for some fundamental biological functions. It is therefore natural that several research groups have focused their studies on the building of supramolecular helices.[2]

The use of nucleobases to build up complex supramolecular structures is being increasingly investigated.[3] Of these bases, guanine (G) appears to be the most versatile as, besides forming the standard GC pair, it is able to self-assemble to give different supramolecular architectures.[4] In particular, depending on the substituents present and the experimental conditions, lipophilic G-derivatives can generate quartets,[5] ribbonlike structures,[6] and, in the presence of metal templates, G-quartet-based aggregates (Figure 1).

Both columnar structures and ribbons can form liquid-crystalline gels with different topologies. Furthermore, columnar structures have recently been proposed as possible ion channels,[7] whereas ribbons on surfaces show interesting electrical properties.[8]

In a recent paper, we reported that 8-oxoguanosine (8-oxoG; **1**), bearing lipophilic substituents on the sugar moiety, forms liquid-crystalline gels in hydrocarbon solvents.[9] 8-Oxoguanosine possesses a rich array of hydrogen-bond donor and acceptor sites, and identifying their possible interactions in the self-assembly process constitutes a diffi-

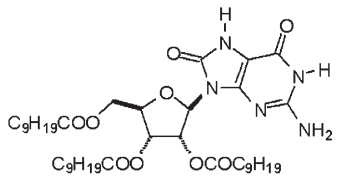

1

[a] S. Lena, Prof. G. Gottarelli, C. Graziano, Dr. S. Masiero, Dr. S. Pieraccini, Prof. G. P. Spada
Alma Mater Studiorum–Università di Bologna
Dipartimento di Chimica Organica "A. Mangini"
Via San Giacomo 11, 40126 Bologna (Italy)
Fax: (+39) 051-209-5688
E-mail: gottarel@alma.unibo.it
GianPiero.Spada@unibo.it

[b] Dr. M. A. Cremonini, Dr. L. Laghi
Alma Mater Studiorum - Università di Bologna
Dipartimento di Scienze degli Alimenti
Piazza Goidanich 60, 47023 Cesena (Italy)

[c] Dr. F. Federiconi, Prof. P. Mariani
Università Politecnica delle Marche
Dipartimento di Scienze Applicate ai Sistemi Complessi
Via Ranieri 65, 60131 Ancona (Italy)

Supporting information for this article is available on the WWW under http://www.chemeurj.org/ or from the author.

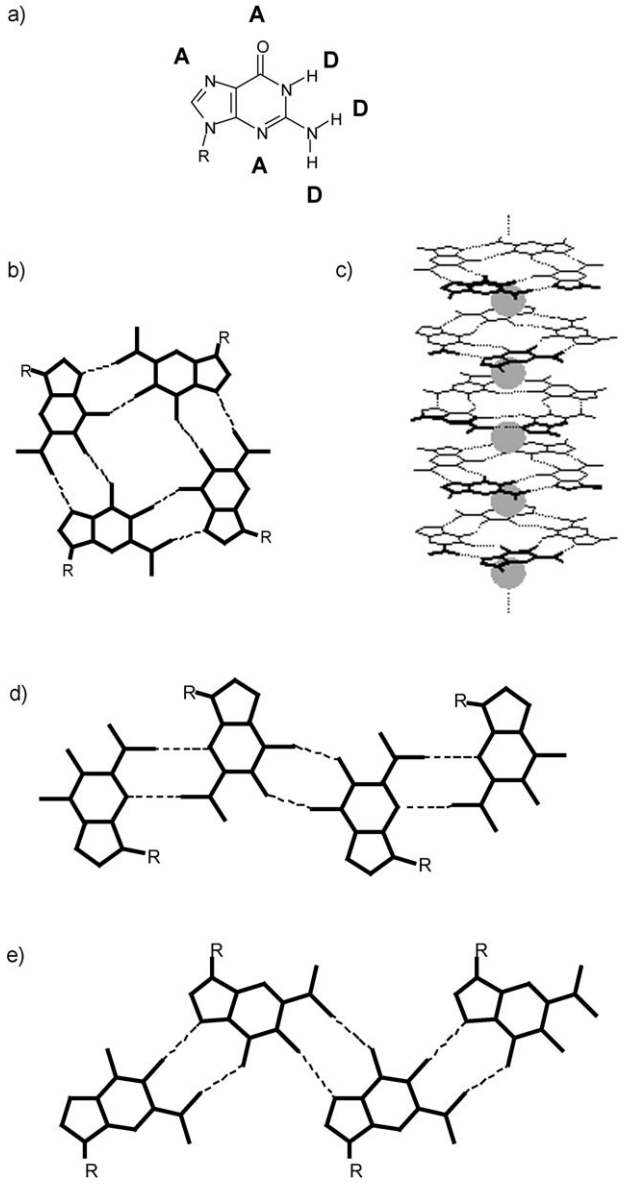

Figure 1. Donor/acceptor sites of the guanine moiety (a), the G-quartet arrangement (b), the columnar G-quartet ion-directed architecture (c), and two different ribbon-like assemblies (d, e) in the absence of cations.

cult task. However, we have obtained strong evidence that the exocyclic amino group is not directly involved in the self-assembly process.[9] Even so, several self-assembled structures can be hypothesized: a ribbon, a cyclic quartet, and a continuous helix. Of the aforementioned structures, we identified the helical architecture as the most populated one for 8-oxoG **1**, both in solution and in the liquid-crystalline phases (Figure 2).

8-Oxoinosine derivatives (8-oxoI; **2**) do not possess the exocyclic amino group and should thus be suitable for checking whether the supramolecular structure assigned to 8-oxoG is correct, even though such subtle modifications may clearly influence the self-assembly processes. In princi-

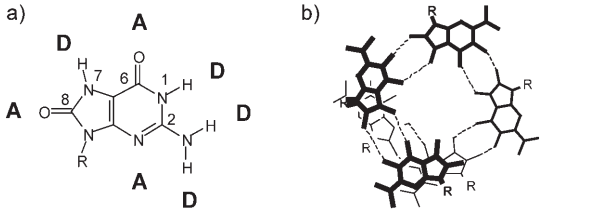

Figure 2. Donor/acceptor groups of the 8-oxoguanine moiety (a) and the helical supramolecular architecture (b).

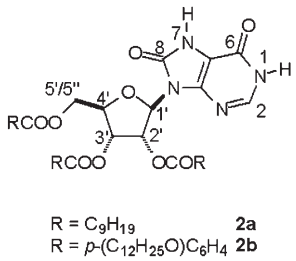

ple, 8-oxoI can self-assemble to give a ribbon, a quartet, or a continuous helix (Figure 3).

Herein, we present supporting evidence for the helical structure assignment by characterizing the solid-state film obtained from derivative **1** by means of small-angle X-ray scattering (SAXS), and we describe the self-assembly of lipophilic 8-oxoI derivatives **2a** and **2b**, and a liquid-crystalline gel formed by **2b** in hydrocarbon solvents. Notably, while derivative **2b**, bearing large substituents on its ribose moiety, undergoes self-assembly and mesophase formation,

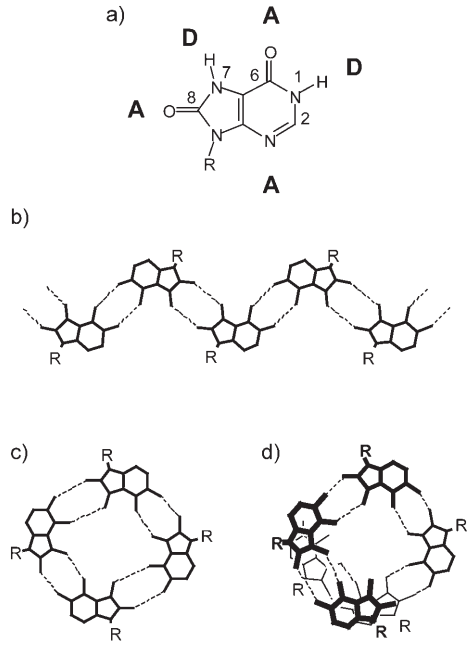

Figure 3. Donor/acceptor groups of the 8-oxoI moiety (a) and three possible supramolecular architectures: a ribbon (b), a cyclic quartet (c), and a continuous helix (d).

8-oxoinosine **2a**, with only decanoyl groups on its ribose moiety, does not. This can be attributed to the reduced amphiphilic properties of the latter.

Results and Discussion

Small-angle X-ray scattering of 8-oxoG 1: As it proved impossible to obtain X-ray quality crystals of the series of 8-oxoguanosine derivatives, we studied the SAXS of the film obtained by spin-drying of a solution of derivative **1** in chloroform.

The X-ray diffraction pattern is shown in Figure 4. According to our previous work,[9] the data are consistent with

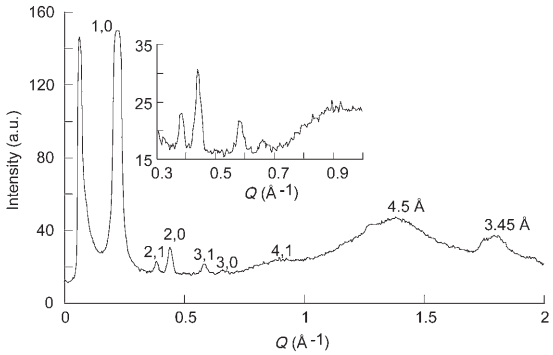

Figure 4. X-ray diffraction profile obtained from a dry film of **1**.

the presence of a hexagonal columnar phase. In particular, the low-angle diffraction region is characterized by a series of at least seven narrow peaks with spacing ratios in the order $1{:}\sqrt{3}{:}\sqrt{4}{:}\sqrt{7}{:}\sqrt{9}{:}\sqrt{12}{:}\sqrt{13}$, which index according to a two-dimensional hexagonal lattice of *p6m* symmetry.[10] From the Bragg spacings $Q_{h,k}$, the unit cell dimension a (that is, the inter-axial distance between the aggregates) has been obtained from Equation (1):[10]

$$a = (4\pi/\sqrt{3})\sqrt{(h^2 + k^2 - hk)}/Q_{h,k} \quad (1)$$

where h and k are the Miller indices of the observed Bragg reflections. In full agreement with the concentration dependence observed in hexane,[9] and as the film is dry, a rather small unit cell dimension of 32.9 Å was derived.

Experimental evidence for the columnar nature of the phase has been obtained by analysis of the high-angle diffraction region. In accordance with previous research,[9,10] a narrow band is observed at about $Q = 1.81\ \text{Å}^{-1}$ (see Figure 4). This band is related to the nature of the order inside the structure elements, which are helical columns composed of 8-oxoG residues stacked almost perpendicularly to the column axis. From the position of this peak, a repeat distance between neighboring 8-oxoguanosines of 3.45 Å is obtained.

The high-angle region is also characterized by a large band, centered at $Q = 1.4\ \text{Å}^{-1}$ (corresponding to a repeat distance of about 4.5 Å), which indicates the disordered conformation of the lipophilic substituents.

From the unit cell, the cross-sectional radius of the helix can be determined by assuming that the columns have a circular section with radius R and are infinite in length. The relationship between the cross-sectional area of the cylinder and the two-dimensional hexagonal unit cell surface is given by Equation (2):[9–11]

$$\pi R^2 = (\sqrt{3}/2)a^2 c_{v,G} \quad (2)$$

where $c_{v,G}$ is the volume concentration of the 8-oxoguanine base inside the unit cell volume. In this special case, in which the solvent is absent, $c_{v,G}$ corresponds to the volume fraction of the 8-oxoguanine residue ($V_G = 372\ \text{Å}^3$) with respect to the molecular volume ($V_{mol} = 1182\ \text{Å}^3$) calculated from standard atomic dimensions, that is $c_v = 0.327$, giving a radius of 9.9 Å.

The structural analysis was further developed by considering the intensities of the Bragg peaks observed in the low-angle diffraction region. The two-dimensional electron-density profile can thus be obtained by calculating the two-dimensional Fourier distribution [Eq. (3)]:[11,12]

$$\rho(x,y) = \sum\nolimits_{h,k} (\pm F_{h,k} \cos(Q_{(x)h,k} x) \cos(Q_{(x)h,k} y)) \quad (3)$$

where $F_{h,k}$ is the Fourier coefficient of the peak at position $Q_{h,k}$, and is related to the peak intensity by $F_{h,k}\ (I_{h,k}/m_{h,k})^{1/2}$, where $m_{h,k}$ is the multiplicity of the h,k reflection. The phase information for each diffraction order is either positive or negative for a centrosymmetric scattering length density profile, such as that pertaining to the hexagonal phase. The correct sign of the Fourier coefficients $F_{h,k}$ has been obtained by considering a geometrical model of the helix.[12] For the sake of simplicity, this model was assumed to be cylindrically symmetric. The unit cell was split into four regions: the central cavity, the 8-oxoguanine region, the sugar residue region, and the hydrocarbon region in which the lipophilic substituents (and possibly also the hydrocarbon solvent) are located, as shown in Figure 5. The model was obtained by adding uniform disks of appropriate density. The Fourier transform of this 2D model is given by the continuous function $F(Q)$ [Eq. (4)]:[12]

$$\begin{aligned} F(Q) &= 2(R_1^2(\rho_1 - \rho_2)J_1(QR_1)/QR_1 \\ &+ R_2^2(\rho_2 - \rho_3)J_1(QR_2)/QR_2 \\ &+ R_3^2(\rho_3 - \rho_0)J_1(QR_3)/QR_3)/(R_1^2(\rho - \rho_2) \\ &+ R_2^2(\rho_2 - \rho_3) + R_3^2(\rho_3 - \rho_0)) \end{aligned} \quad (4)$$

where J_1 is the first-order Bessel function of the first kind; ρ_1, ρ_2, and ρ_3 are the electron densities of the central cavity, the 8-oxoguanine, and the sugar residue, respectively, and ρ_0 is the average electron density of the hydrocarbon region. Moreover, R_1 is the radius of the central hole, R_2 is the

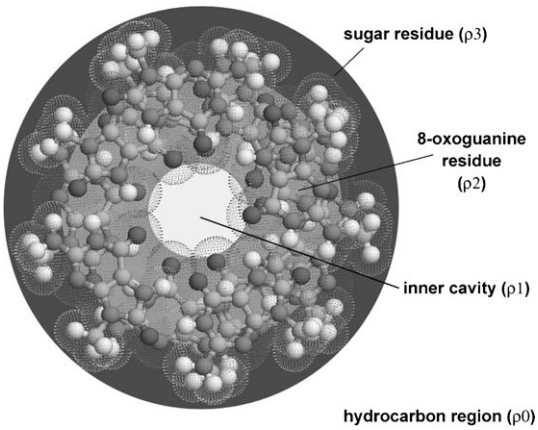

Figure 5. Section of the cylindrically symmetric geometrical model used to represent the aggregate.

outer radius of the 8-oxoguanine shell, and R_3 is the outer radius of the shell within which the sugar residues are located. Dimensions and scattering length densities used in the model, as derived from molecular models and chemical compositions, were as follows: $R_1 = 1.5$ Å, $R_2 = 7$ Å, $R_3 = 12$ Å, $\rho_1 = 0.33\,\mathrm{e\,Å^{-3}}$, $\rho_2 = 0.46\,\mathrm{e\,Å^{-3}}$, $\rho_3 = 0.47\,\mathrm{e\,Å^{-3}}$, and $\rho_0 = 0.27\,\mathrm{e\,Å^{-3}}$. The corresponding $F(Q)$ continuous function is shown in the Supporting Information. Even though the soft and disordered nature of these systems may seriously affect the model structure,[11] the derived continuous function can be used to set the signs of the experimental Fourier coefficients in order to directly calculate the electron density map by applying Equation (3).

The electron density distribution is shown in Figure 6. The circular 8-oxoG contour can be readily appreciated, but other important features are also evident, such as the presence of the hole in the central region of the helix, the approximately constant density corresponding to the tetrameric contour region, and the flat electron density in regions far away from the cylinder surfaces. The outer radius of the 8-oxoguanine shell can be directly measured from the map as 10.5 Å. The very good agreement between the helix radius calculated from the unit cell dimension and molecular volumes (9.9 Å; see above) and that measured from the map is noteworthy.

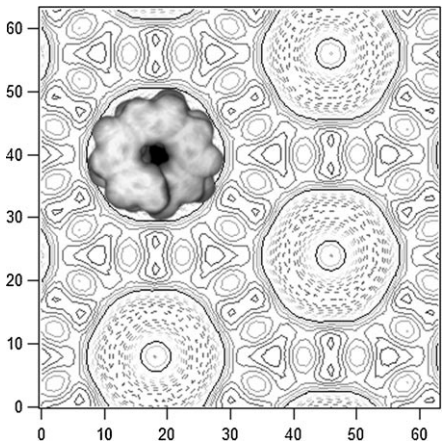

Figure 6. Calculated electron density distribution for a dry film of **1**. The normalized Fourier coefficients are as follows: $F_{1,0} = 0.313$; $F_{2,1} = -0.100$; $F_{2,0} = -0.163$; $F_{3,1} = -0.090$; $F_{3,0} = -0.080$; $F_{4,2} = 0.0$; $F_{4,1} = 0.068$ (diffracted intensities are normalized such as $\Sigma_{h,k} I_{h,k} = 1.0$, so that the map shows the fluctuation of the electron density around the average value, set to 0). The density levels are equally spaced, with an increment of 0.2: dashed and full lines represent positive and negative levels, respectively. Axis dimensions are in ångströms.

Synthesis and self-assembly of 8-oxoI 2: In the helix proposed for 8-oxoG, the 2-amino group does not participate directly in the hydrogen-bond framework between the bases that generate the helical structure.[9] We have therefore synthesized two lipophilic 8-oxoinosines to see if we could still obtain assembled structures and liquid-crystalline gels. Derivatives **2a** and **2b** were prepared according to Scheme 1.

Commercial adenosine (**3**) was brominated at the 8-position with bromine in sodium acetate buffer. The resulting 8-bromoadenosine **4** was diazotized with $NaNO_2$ in acetic acid at room temperature and the resulting diazonium salt was hydrolyzed in situ to afford 8-bromoinosine **5**. Derivative **5** was then converted to triacetyl 8-oxoinosine **6** by substitution of bromine with acetate in acetic acid/acetic anhydride at 160 °C and subsequent hydrolysis of the resulting enol ester. Subsequent transesterification with sodium methoxide in methanol at 50 °C gave 8-oxoinosine **7**. This compound was esterified with the appropriate anhydride or aroyl chloride in MeCN at room temperature to afford **2a** and **2b**, respectively.

In contrast to derivative **1**, which exhibits two liquid-crystalline phases in hydrocarbon solvents,[9] solutions of derivative **2a** do not show any birefringence up to about 80 % w/w in either hexane or chloroform. Furthermore, in the same solvents, the circular dichroism spectra of **2a** show only weak signals corresponding to the 8-oxoinosine chromophore (see Supporting Information). The shape and intensity of the CD spectrum suggest the absence of a helicoidal order in the supramolecular structure. Finally, the ^{1}H NMR spectrum in $CDCl_3$ is quite similar to that in DMSO (in which H-bonded architectures are not expected to exist); that is to say, there is no notable shift of the resonances or variation of band widths with the change of solvent.

The different behavior of **2a** and **1** may be attributed to solvophobic effects. The lyomesomorphism requires that the molecules are amphiphilic: the driving force of the self-assembly derives from the segregation of the different parts of the molecules, such that in the self-assembled species, the lyophilic part is exposed to the solvent, while the lyophobic part is not in contact with the solvent. The absence of the amino group in **2a** decreases the lyophobic character of the aromatic base and this reduces the amphiphilic properties of **2a** and hence its propensity to give large supramolecular structures and consequently lyotropic mesophases.

Self-assembly of 8-oxoI 2b to give a liquid-crystalline phase: To ascertain whether increasing the amphiphilicity of the ox-

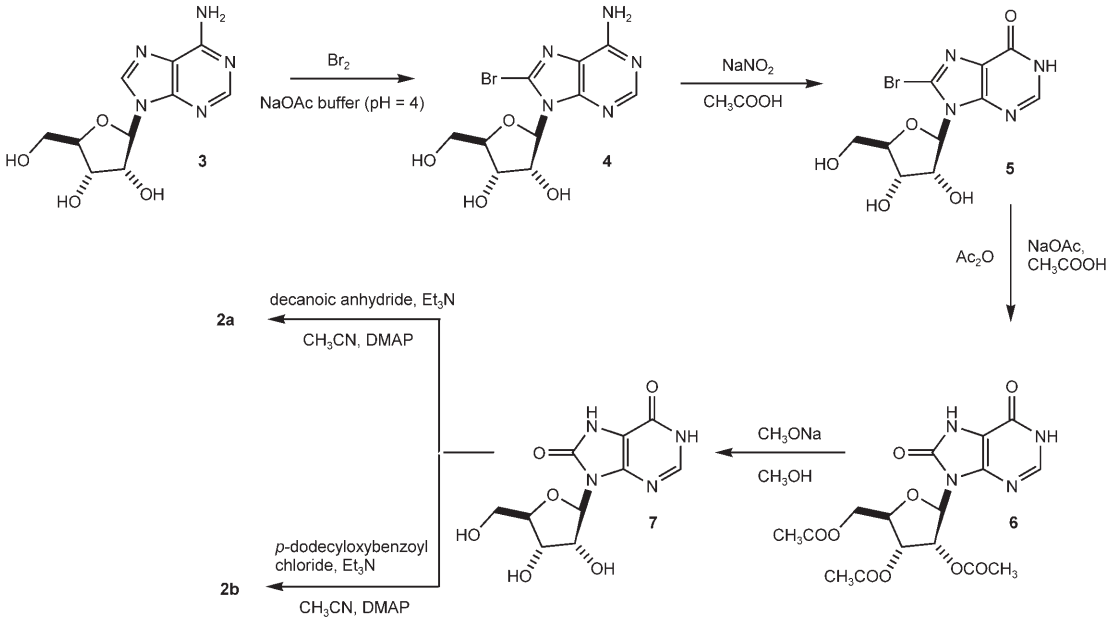

Scheme 1. Synthetic route to **2a** and **2b**.

oinosine derivative would increase its ability to self-assemble, we prepared compound **2b** (see Scheme 1). In this derivative, aromatic groups and longer alkyl chains are present on each of the three tails exposed to the solvent as compared to the substituents on **2a**. This structural feature should increase the difference in lyophilicity between the core (the 8-oxohypoxanthine base) and the rest of the molecule. Furthermore, there may be stabilizing interactions between the aromatic groups. In fact, it has recently been reported that aromatic side chains considerably enhance the stability of double-helical foldamers.[13] Compound **2b** was indeed found to exhibit lyotropic liquid-crystalline properties in hydrocarbon solvents. Optical microscopy revealed the presence of a birefringent fluid phase at $c > 2.3\,\%$ and 3.5% in hexadecane and heptane, respectively (where c is the ratio of the weight of **2b** to the total weight of the sample) (Figure 7).

X-ray diffraction experiments confirmed the existence of a liquid-crystalline order that is only clearly detectable at high concentration. Thus, at concentrations higher than 15%, a series of diffraction peaks was seen in the X-ray profile. The characteristic peak positions confirmed the liquid-crystalline nature of the sample (Figure 8). The low-angle

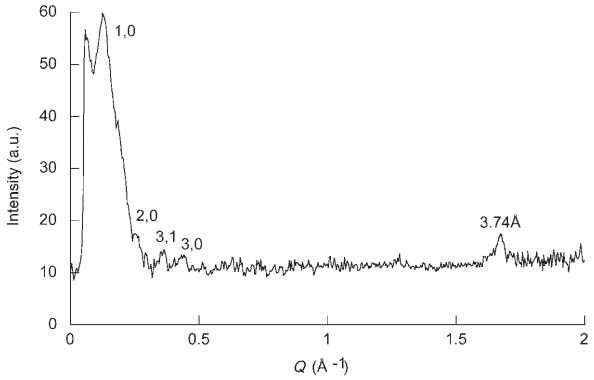

Figure 8. X-ray diffraction profile obtained from a 30% (w/w) solution of **2b** in heptane.

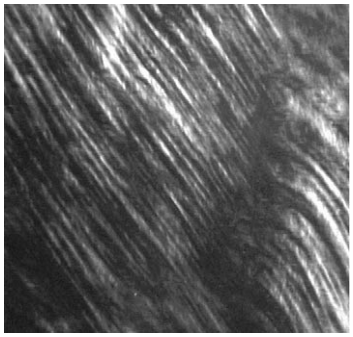

Figure 7. Polarized optical microscopy image of a 10% (w/w) solution of **2b** in hexadecane. Magnification 100×.

X-ray diffraction region is dominated by a strong peak, the position of which depends on the solvent concentration, while higher order diffraction peaks can only be detected after very long exposure times. Under optimal conditions, two or three further peaks were detected, which helped in the assessment of the lattice symmetry.[9,10] The observed peak reciprocal spacings were in the ratio $1:\sqrt{3}:\sqrt{4}:\sqrt{7}:\sqrt{9}$, indicating a two-dimensional hexagonal packing of the structural elements.

A characteristic peak, centered at about 3.74 Å ($Q = 1.68\,\text{Å}^{-1}$), was observed in the high-angle region, the position of which was independent of the concentration. The presence of this peak indicates the columnar nature of the

aggregates of **2b** [9,10] and suggests that the stacked bases may be arranged in a helical fashion, as observed for derivative **1**.[9] Assuming that the stacking distance between the 8-oxoinosine residues is again the standard 3.4 Å, the observed 3.74 Å peak suggests that the angle formed by the bases in relation to a plane perpendicular to the column axis is around 23°. As in the case of derivative **1**, the high-angle region is also characterized by a large band at $Q = 1.4$ Å^{-1}, which is related to the disordered conformation of the lipophilic substituents in the hydrocarbon region.

Two points were then considered: first, the dependence of the inter-helix distance on the sample composition, and second, the reconstruction of the electron density distribution. Figure 9 shows the unit cell dimension measured for

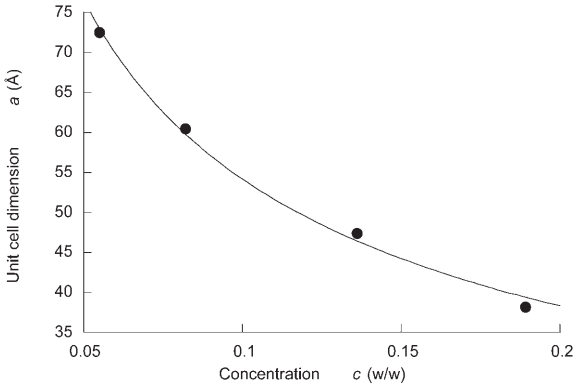

Figure 9. Dependence on concentration of the 2D hexagonal unit cell dimension for **2b**.

the hexagonal phase as a function of the concentration: interestingly, the concentration dependence of the unit cell dimension is $c_{v,G}{}^{-1/2}$ and consequently the swelling behavior appears to be well described by a model composed of rod-like elements of infinite length that move apart as dilution proceeds (2D swelling, see reference [9]). By fitting the data by using Equation (2), a radius of 9 Å was derived for the cross-section of the 8-oxoinosine helices (only the aromatic core 8-oxohypoxanthine was considered). Electron density distributions have been calculated by using Equation (3) and the sign of the Fourier coefficients $F_{h,k}$ was obtained by considering the helical geometric model described above. The electron density map for the 8-oxoI derivative **2b** at $c = 0.3$ is presented in Figure 10: comparison with the map obtained for sample **1** clearly illustrates the lower experimental resolution (for example, no details concerning the central cavity are visible) and the swelling determined by the solvent. Nevertheless, the similar shape and size of the cross-sections of the two helices can be readily appreciated (see Table 1).

Self-assembly of 8-oxoI 2b to give an isotropic solution: To obtain information on the structure of the supramolecular aggregates arising from **2b** in isotropic solution, a comparative NMR study was carried out in chloroform and DMSO

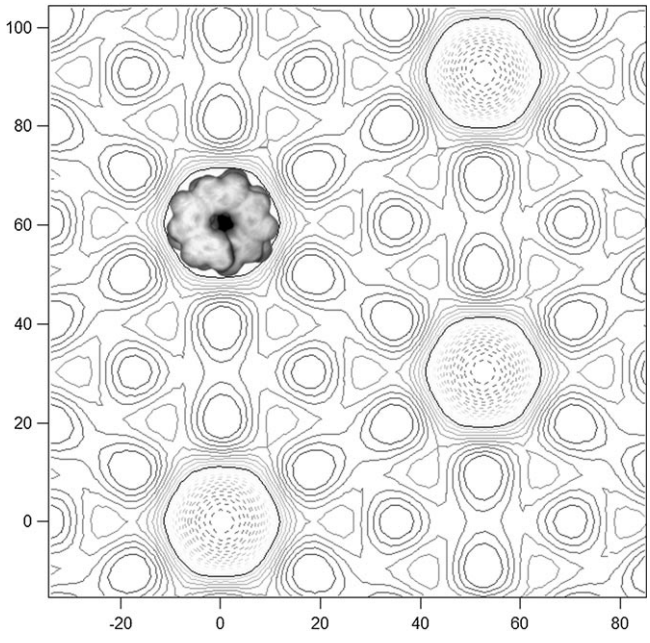

Figure 10. Calculated electron density distribution for the mesophase of **2b** ($c = 0.3$). The normalized Fourier coefficients are as follows: $F_{1,0} = 0.319$; $F_{2,1} = 0.192$; $F_{2,0} = 0.092$; $F_{3,1} = 0.067$; $F_{3,0} = -0.102$ (diffracted intensities are normalized such as $\Sigma_{h,k} I_{h,k} = 1.0$, so that the map shows the fluctuation of the electron density around the average value, set to 0). The density levels are all equally spaced, with an increment of 0.2: dashed and full lines represent positive and negative levels, respectively. Axis dimensions are in ångströms.

Table 1. Structural data of the mesophases formed by **2b** in heptane at different weight concentrations (c). R is the cross-sectional radius of the helix calculated from unit cell dimensions and sample concentration ([Eq. (2)]); R' is the outer radius of the 8-oxohypoxanthine shell directly measured from the electron density maps.

c	$c_{v,G}$	a [Å]	R	R'
0.2	0.055	72.6	8.9	10.5
0.3	0.082	60.5	9.1	10.5
0.5	0.136	47.4	9.2	10.5
0.7	0.189	38.2	8.7	10.5

solutions, the latter being a strongly competing solvent for hydrogen bonding.

The ^{1}H NMR spectrum of **2b** in [D$_6$]DMSO at room temperature (25 °C) shows a single series of peaks (see Supporting Information), the assignments for which are presented in Table 2.

Each proton gives rise to a peak of roughly the same width, with the exception of the NH(1) and NH(7) protons, the peaks due to which are approximately seven times broader. The ^{1}H NMR spectrum of **2b** in $CDCl_3$ at room temperature also shows a single series of peaks. Notably, however, the signals are significantly broader than those observed in [D$_6$]DMSO: in particular, the signals due to H(2), the sugar residue protons, and the NH protons are 10, 20, and 40–50 times broader, respectively. The existence of aggregates large enough to give rise to broad signals was ruled out by means of an external reference.

Table 2. ^{1}H NMR (400 MHz) chemical shifts for a 13 mM solution of **2b** (25 °C). Assignments were made on the basis of COSY, NOESY, and ROESY spectra.

Solvent	NH(1)	NH(7)	H(2)	H(1′)	H(2′)	H(3′)	H(4′)	H(5′/5″)[a]	Ph protons
$CDCl_3$	12.39	11.20	7.81	6.35	6.53	6.16	4.70	4.77, 4.67	8.07–7.84, 6.82
$[D_6]$DMSO	12.68	11.59	7.92	6.07	6.30	6.04	4.65	4.59, 4.48	7.88–6.88

[a] Diastereotopic protons have not been assigned.

In principle, proof of the aggregation of **2b** in $CDCl_3$ could be obtained by comparing the sign of the NOESY cross-peaks with respect to the diagonal in $[D_6]$DMSO and $CDCl_3$. However, this was not possible in our case as **2b** displayed NOESY cross-peaks with the *same* sign as the diagonal in both solvents (i.e., $\omega\tau_c > 1.12$ even in DMSO), due to its high molecular mass ($M_w = 1149.50$). Indirect proof of aggregation has nevertheless been obtained from analysis of ROESY spectra, which were preferred to NOESY spectra because of the possibility of distinguishing between a cross-peak generated by a direct through-space interaction and one due to relayed ROE or chemical exchange, regardless of τ_c.[14]

In principle, two modes of assembly may be adopted in solution: one based on hydrogen bonding between the NH(7)-CO(8) amide group of one molecule and the NH(1)-CO(6) amide group of another molecule, the other based on hydrogen bonding between two NH(7)-CO(8) amide groups of two molecules and between two NH(1)-CO(6) amide groups of two molecules. The first possibility leads to G-quartet-like or helical ribbon superstructures, while the latter gives rise to a linear self-assembled ribbon (see Figure 3).

To ascertain whether the supramolecular arrangement at high concentration inferred from the X-ray diffraction experiments persists in isotropic solution, we realized that, according to models, such an arrangement implies an intermolecular distance between NH(7) of an inosine moiety and H(2) of another inosine located at a different level of the supramolecular helix that is shorter than the intramolecular distance of 5.9 Å. Thus, if a helical structure is present, a ROESY cross-peak should be detected between the NH(7) and H(2) signals in chloroform (but not in DMSO), provided that the spin lock is kept sufficiently short to avoid significant NH(7) magnetization decay with $T_{1\rho}$. ROESY spectra were thus run with a very short mixing time of 15 ms, similarly to experiments reported in the literature in the presence of rapidly relaxing protons.[15] Our ROESY results are consistent with the existence of a supramolecular structure in $CDCl_3$. The required cross-peak between NH(7) and H(2) is indeed only observed in $CDCl_3$ solution (see Supporting Information), its positive sign (negative diagonal) confirming that it is due to a genuine ROE. Taken alone, this finding does not prove that a helical structure is adopted in solution, but it definitely rules out the possibility of a ribbon architecture in chloroform.

A ROESY spectrum obtained from a solution of **2b** in DMSO using a longer mixing time (200 ms) showed positive cross-peaks between protons separated by one carbon–carbon bond, as well as cross-peaks between protons H(1′) and H(4′) and between protons H(3′) and H(5′)/H(5″). The corresponding spectrum obtained from a solution in $CDCl_3$ showed substantially the same cross-peak pattern, but with one salient difference, namely a positive, medium-intensity cross-peak between H(1′) and both the H(5′) and H(5″) protons. The presence of this cross-peak seems to rule out the linear ribbon structure (and supports a helical or a stacked G-quartet-like structure). An intramolecular ROE seems to be excluded due to the excessive distance of three C–C bonds; a spin diffusion effect also seems unlikely. Spin diffusion through H(4′) would give a negative cross-peak between H(1′) and H(5′)/H(5″), while the observed cross-peak is positive. A doubly relayed ROE would give a cross-peak with the correct sign, but considering that the sample was not degassed and that the intensity of cross-peaks between protons separated by single C–C bonds is weak, this possibility seems remote. Finally, an intermolecular ROE seems to be excluded in the case of a linear assembly, due to the clearly excessive distance.

We therefore conclude that the above-mentioned NOE coupling arises from hydrogens belonging to nucleosides in a partially stacked configuration (see Figure 11), as is the case in a continuous, helical ribbon or a stacked G-quartet-like structure. It should be noted that in previous examples of stacked G-quartets in the presence of ions,[16] two sets of proton signals were observed.

Figure 11. A molecular sketch of a fragment of the supramolecular helix of **2b.** ROE contacts H(1′)–H(5′/5″) and H(2)–NH(7) are indicated by lines.

CD spectra of **2b** in different solvents are presented in Figure 12. This compound exhibits a first intense absorption band at around 250–260 nm (with a shoulder at ca. 275 nm) and a second band at around 215 nm. In methanol (in which H-bonded guanine architectures are generally absent), the CD spectrum features weak signals in both wavelength re-

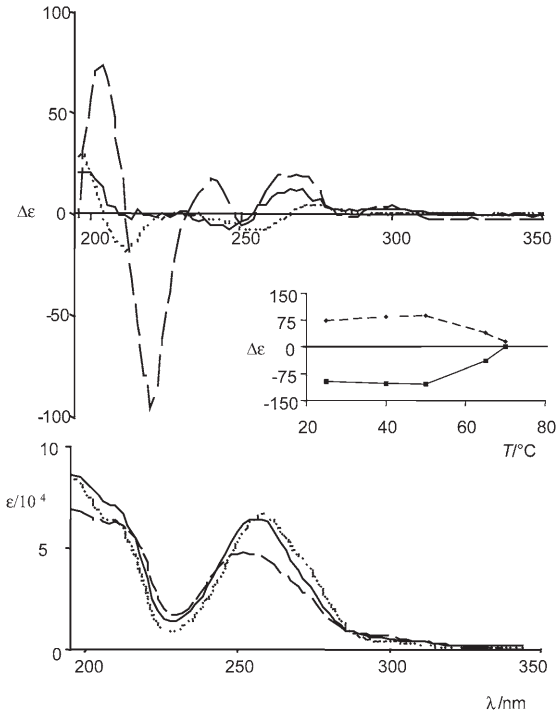

Figure 12. CD (top) and absorption (bottom) spectra of a 1-mM solution of **2b** in methanol (25 °C, dotted line) and in cyclohexane at 25 °C (dashed line) and 70 °C (solid line). In the inset: the melting profile in cyclohexane monitored at 203 nm (dashed line) and 220 nm (solid line).

gions. In contrast, the CD spectrum in hydrocarbon solvents shows a much stronger signal in the region 230–280 nm and a very intense ($\Delta\Delta\varepsilon \approx 170$; $\Delta\varepsilon/\varepsilon \approx 2\times10^{-3}$), exciton-like, bisignate couplet centered at 215 nm. This spectrum does not change with concentration in the range 0.01–1 mM, indicating that the structure of the species in solution is not affected by concentration. On increasing the temperature, the shape of the CD spectrum of a 1 mM solution changes dramatically and at 70 °C the exciton couplet at 215 nm has almost completely vanished. As no assignment of the electronic transitions of the 8-oxohypoxanthine chromophore is available and, furthermore, in derivative **2b** the benzoyl chromophore also contributes to the CD, detailed analysis of the spectrum is not possible. However, a few issues may be considered: 1) that different CD spectra are obtained in cyclohexane and methanol resembles the behavior of 8-oxoG **1**;[9] 2) the intensity of the CD signal and the g-factor ($\Delta\varepsilon/\varepsilon$) in cyclohexane are only compatible with a "highly" chiral structure, much more so than the chiral structures composed of stacked G-quartets.

Conclusions

Considering that 1) the G-quartets are unable to stack in the absence of metal ions,[5] 2) the anisotropy factor, *g*, is much higher than those of chiral structures composed of stacked G-quartets,[9] and 3) the ^{1}H NMR spectra show only a single set of signals whereas columnar structures of stacked, metal-templated G-quartets show multiple sets[16] (and this should also apply to possible columns without metal ions), we believe that a continuous helical architecture is most likely adopted by 8-oxoI **2b** (Figure 3d). The situation is analogous to that reported for 8-oxoG, the assembled structure of which has been confirmed in this work by SAXS measurements on a film.

Experimental Section

General: CD spectra were recorded on a JASCO J-710 spectropolarimeter using cells of the appropriate pathlength. NMR spectra were recorded on Varian Mercury instruments at 300 or 400 MHz. X-ray diffraction experiments were performed using a Philips PW1830 X-ray generator equipped with a Guinier-type focusing camera operating in a vacuum; a bent quartz crystal monochromator was used to select $Cu_{K\alpha1}$ radiation (λ = 1.54 Å). The investigated Q range ($Q = (4\pi \sin\theta)/\lambda$, where 2θ is the full scattering angle) was between 0.068 and 2.3 Å^{-1}. Diffraction patterns were recorded on a stack of two Kodak DEF-392 films; film densities were measured by using a digital scanner and scattered intensities were corrected for electronic noise and sample holder signals. For data evaluation purposes, Bragg peaks were fitted by Lorentzian distributions and peak intensities $I_{h,k}$ (h,k are the reflection indices) were obtained by multiplying each peak area by its corresponding wave vector $(Q/2\pi)^2$ (for a discussion, see reference [17]).

2′,3′,5′-*O*-Tridecanoyl-8-oxoguanosine (**1**) was prepared according to reference [9]. 2′,3′,5′-*O*-Tridecanoyl-8-oxoinosine (**2a**) and 2′,3′,5′-*O*-tris(4-dodecyloxybenzoyl)-8-oxoinosine (**2b**) were prepared starting from commercial **3** (see Scheme 1) according to the procedures outlined below. Derivatives **4**, **5**, and **6** were synthesized as reported in references [18], [19], and [20], respectively. 4-(Dodecyloxy)benzoyl chloride was prepared according to standard procedures.

8-Oxoinosine (7): Na (0.35 g, 15 mmol) was dissolved in anhydrous methanol (15 mL) and the resulting methoxide solution was combined with compound **6** (1.50 g, 3.80 mmol). The product precipitated immediately, and after 2 h the solid was isolated by filtration to give **7** (0.54 g; 50 % yield). ^{1}H NMR (300 MHz, [D$_6$]DMSO): δ = 3.40–3.70 (m, 2H; H5′/H5″), 3.84 (m, 1H; H4′), 4.10 (m, 1H; H3′), 4.82 (m, 1H; H2′), 5.64 (dd, 1H; H1′), 7.89 ppm (s, 1H; ArH, H2).

2′,3′,5′-*O*-Tridecanoyl-8-oxoinosine (2a): 8-Oxoinosine (0.3 g, 1.0 mmol) was dried over P_2O_5 in vacuo for 2 h at 50 °C and then suspended in anhydrous acetonitrile (8 mL). Redistilled Et_3N (0.5 mL, 3.6 mmol), decanoic anhydride (1.2 mL, 3.3 mmol), and a catalytic amount of DMAP were added, and the resulting mixture was stirred overnight. After evaporation of the solvent in vacuo, the crude material was applied to a column of silica gel. After washing with dichloromethane/acetone (95:5) to remove the decanoic acid, 2′,3′,5′-*O*-tridecanoyl-8-oxoinosine was eluted with dichloromethane/methanol (96:4). The solvents were evaporated in vacuo to afford **2a** (0.56 g; 76 % yield). ^{1}H NMR (300 MHz, [D$_6$]DMSO): δ = 0.84 (m, 9H; CH_3), 1.23 (m, 36H; CH_2), 1.49 (m, 6H; OC-CH_2CH_2), 2.30 (m, 6H; OC-CH_2), 4.12–4.22 (m, 2H; H5′/H5″), 4.33 (m, 1H; H4′), 5.58 (m, 1H; H3′), 5.81 (dd, 1H; H1′), 6.01 (m, 1H; H2′), 8.00 (s, 1H; ArH, H2), 11.61 (brs, 1H; NH), 12.60 ppm (brs, 1H; NH); ^{13}C NMR (75 MHz, $CDCl_3$): δ = 14.29 (CH_3), 14.44 (CH_3), 22.93 (CH_2), 25.05 (CH_2), 25.11 (CH_2), 25.83 (CH_2), 29.55 (CH_2), 29.69 (CH_2), 32.13 (CH_2), 34.15 (CH_2), 34.20 (CH_2), 34.28 (CH_2), 35.94 (CH_2), 63.70 (CH_2), 70.79 (CH), 71.80 (CH), 79.94 (CH), 84.76 (CH), 109.62 (C), 144.30 (C), 144.51 (C), 145.66 (CH), 152.73 (C), 172.63 (C), 172.72 (C), 173.78 ppm (C); elemental analysis calcd (%) for $C_{40}H_{66}N_4O_9$: C 64.32, H 8.91, N 7.50; found: C 64.46, H 9.29, N 7.59.

2′,3′,5′-*O*-Tris(*p*-dodecyloxybenzoyl)-8-oxoinosine (2b): 8-Oxoinosine (0.20 g, 0.7 mmol) was dried over P_2O_5 in vacuo for 2 h at 50 °C and then suspended in anhydrous acetonitrile (6 mL). Redistilled Et_3N (0.35 mL, 2.51 mmol), 4-(dodecyloxy)benzoyl chloride (0.75 g, 2.31 mmol), and a catalytic amount of DMAP were added. The mixture was stirred over-

night. The reaction was stopped by adding methanol (2 mL) and, after evaporation of the solvent in vacuo, the crude material was crystallized from ethanol/chloroform to afford **2b** as a white solid (0.54 g; 68% yield). ^{1}H NMR (300 MHz, [D$_6$]DMSO): δ = 0.84 (m, 9H; CH$_3$), 1.23 (m, 48H; CH$_2$), 1.38 (m, 6H; O-CH$_2$CH$_2$CH$_2$), 1.69 (m, 6H; O-CH$_2$CH$_2$), 4.01 (m, 6H; O-CH$_2$), 4.46–4.70 (m, 3H; H4′, H5′, and H5″), 6.06 (m, 1H; H3′), 6.09 (d, 1H; H1′), 6.32 (dd, 1H; H2′), 6.88–7.02 (m, 6H; ArH), 7.74–7.95 (m, 7H; ArH), 11.61 (s, 1H; NH), 12.70 ppm (s, 1H; NH); ^{13}C NMR (100 MHz, [D$_6$]DMSO, 50°C): δ = 14.09 (CH$_3$), 22.30 (CH$_2$), 25.67 (CH$_2$), 28.75 (CH$_2$), 28.80 (CH$_2$), 28.93 (CH$_2$), 29.20 (CH$_2$), 29.24 (CH$_2$), 31.53 (CH$_2$), 63.28 (CH$_2$), 68.22 (CH$_2$), 70.86 (CH), 72.35 (CH), 78.66 (CH), 84.49 (CH), 109.14 (C), 114.49 (CH), 114.60 (CH), 114.76 (CH), 120.77 (C), 120.95 (C), 121.65 (C), 131.55 (CH), 131.67 (CH), 131.83 (CH), 143.93 (C), 145.33 (CH), 151.10 (C), 151.48 (C), 163.03 (C), 163.23 (C), 163.37 (C), 164.51 (C), 165.34 ppm (C); elemental analysis calcd (%) for $C_{67}H_{96}N_4O_{12}$: C 70.01, H 8.42, N 4.87; found: C 70.09, H 8.18, N 4.70.

Acknowledgement

This work has been supported by the MUR/PRIN project Modellazione e caratterizzazione di cristalli liquidi per strutture nano-organizzate (2005035119), the MUR/FIRB project NOMADE (RNNE01YSR8_004), and the University of Bologna.

[1] J.-M. Lehn, *Science* **2002**, *295*, 2400; V. Balzani, A. Credi, F. M. Raymo, J. F. Stoddart, *Angew. Chem.* **2000**, *112*, 3484; *Angew. Chem. Int. Ed.* **2000**, *39*, 3348; S. I. Stupp, V. LeBonheur, K. Walker, L. S. Li, K. E. Huggins, M. Keser, A. Amstutz, *Science* **1997**, *276*, 384.

[2] A. E. Rowan, R. J. M. Nolte, *Angew. Chem.* **1998**, *110*, 65; *Angew. Chem. Int. Ed.* **1998**, *37*, 63; J. C. Nelson, J. G. Saven, J. S. Moore, P. G. Wolynes, *Science* **1997**, *277*, 1793; V. Berl, I. Huc, R. G. Khoury, M. J. Krische, J.-M. Lehn, *Nature* **2000**, *407*, 720; L. J. Prins, T. Timmerman, D. N. Reinhoudt, *J. Am. Chem. Soc.* **2001**, *123*, 10153; D. T. Bong, T. D. Clark, J. R. Granja, M. R. Ghadiri, *Angew. Chem.* **2001**, *113*, 1016; *Angew. Chem. Int. Ed.* **2001**, *40*, 988; ; K. E. S. Phillips, T. J. Katz, S. Jockusch, A. J. Lovinger, N. J. Turro, *J. Am. Chem. Soc.* **2001**, *123*, 11899; H. Fenniri, P. Mathivanan, K. L. Vidale, D. M. Sherman, K. Hallenga, K. V. Wood, J. G. Stowell, *J. Am. Chem. Soc.* **2001**, *123*, 3854; R. Oda, I. Huc, M. Schutz, S. J. Candau, F. C. MacKintosh, *Nature* **1999**, *399*, 566; G. W. Orr, L. J. Barbour, J. L. Atwood, *Science* **1999**, *285*, 1049; V. Percec, M. Glodde, T. K. Bera, Y. Miura, I. Shiyanovskaya, K. D. Singer, V. S. K. Balagurusamy, P. A. Heiney, I. Schnell, A. Rapp, H.-W. Spiess, S. D. Hudson, H. Duan, *Nature* **2002**, *419*, 384; M. L. Bushey, A. Hwang, P. W. Stephens, C. Nuckolls, *Angew. Chem.* **2002**, *114*, 2952; *Angew. Chem. Int. Ed.* **2002**, *41*, 2828; ; A. P. H. J. Schenning, A. F. M. Kilbinger, F. Biscarini, M. Cavallini, H. J. Cooper, P. J. Derrick, W. J. Feast, R. Lazzaroni, P. Leclere, L. A. McDonell, E. W. Meijer, S. C. J. Meskers, *J. Am. Chem. Soc.* **2002**, *124*, 1269; H. Engelkamp, S. Middelbeek, R. J. M. Nolte, *Science* **1999**, *284*, 785; J. H. K. K. Hirschberg, L. Brunsveld, A. Ramzi, J. A. J. M. Vekemans, R. P. Sijbesma, E. W. Meijer, *Nature* **2000**, *407*, 167.

[3] T. Shimizu, R. Iwaura, M. Masuda, T. Hanada, K. Yase, *J. Am. Chem. Soc.* **2001**, *123*, 5947; Z. Li, C. A. Mirkin, *J. Am. Chem. Soc.* **2005**, *127*, 11568; S. Sivakova, S. J. Rowan, *Chem. Soc. Rev.* **2005**, *34*, 9; L. Brunsveld, B. J. B. Folmer, E. W. Meijer, R. P. Sijbesa, *Chem. Rev.* **2001**, *101*, 4071; S. Sivakova, J. Wu, C. J. Campo, P. T. Mather, S. J. Rowan, *Chem. Eur. J.* **2006**, *12*, 446; K. Araki, I. Yoshikawa, *Top. Curr. Chem.* **2005**, *256*, 133.

[4] J. T. Davis, *Angew. Chem.* **2004**, *116*, 684; *Angew. Chem. Int. Ed.* **2004**, *43*, 668; J. T. Davis, G. P. Spada, *Chem. Soc. Rev.* **2007**, DOI: 10.1039/b600282j; G. Gottarelli, G. P. Spada, *Chem. Rec.* **2004**, *4*, 39; G. Gottarelli, G. P. Spada, A. Garbesi, in *Comprehensive Supramolecular Chemistry, Vol. 9, Templating, Self-Assembly and Self-Organization* (Eds.: J.-M. Lehn, J. L. Atwood, D. D. MacNicol, J. A. D. Davies, F. Vögtle, J.-P. Sauvage, M. W. Hosseini), Pergamon, Oxford, **1996**, pp. 483–506; A. Ghoussoub, J.-M. Lehn, *Chem. Commun.* **2005**, *46*, 5763; N. Sreenivasachary, J.-M. Lehn, *Proc. Natl. Acad. Sci. USA* **2005**, *102*, 5938; A. B. Kotlyar, N. Borovok, T. Molotsky, H. Cohen, E. Shapir, D. Porath, *Adv. Mater.* **2005**, *17*, 1901.

[5] J. L. Sessler, M. Sathiosatham, K. Doerr, V. Lynch, K. A. Abboud, *Angew. Chem.* **2000**, *112*, 1356; *Angew. Chem. Int. Ed.* **2000**, *39*, 1300; ; F. W. Kotch, V. Sidorov, Y.-F. Lam, K. J. Kayser, H. Li, M. S. Kaucher, J. T. Davis, *J. Am. Chem. Soc.* **2003**, *125*, 15140; T. N. Pham, S. Masiero, G. Gottarelli, S. P. Brown, *J. Am. Chem. Soc.* **2005**, *127*, 16018.

[6] K. Araki, R. Takasawa, I. Yoshikawa, *Chem. Commun.* **2001**, 1826; T. Sato, M. Seko, R. Takasawa, I. Yoshikawa, K. Araki, *J. Mater. Chem.* **2001**, *11*, 3018; K. Araki, M. Abe, A. Ishizaki, T. Ohya, *Chem. Lett.* **1995**, 359; G. Gottarelli, S. Masiero, E. Mezzina, S. Pieraccini, J. P. Rabe, P. Samorì, G. P. Spada, *Chem. Eur. J.* **2000**, *6*, 3242; T. Giorgi, F. Grepioni, I. Manet, P. Mariani, S. Masiero, E. Mezzina, S. Pieraccini, L. Saturni, G. P. Spada, G. Gottarelli, *Chem. Eur. J.* **2002**, *8*, 2143.

[7] S. L. Forman, J. C. Fettinger, S. Pieraccini, G. Gottarelli, J. T. Davis, *J. Am. Chem. Soc.* **2000**, *122*, 4060; M. S. Kaucher, W. A. Harrell, Jr., J. T. Davis, *J. Am. Chem. Soc.* **2006**, *128*, 38.

[8] G. Maruccio, P. Visconti, V. Arima, S. D'Amico, A. Biasco, E. D'Amone, R. Cingolani, R. Rinaldi, S. Masiero, T. Giorgi, G. Gottarelli, *Nano Lett.* **2003**, *3*, 479; R. Rinaldi, E. Branca, R. Cingolani, S. Masiero, G. P. Spada, G. Gottarelli, *Appl. Phys. Lett.* **2001**, *78*, 3541; R. Rinaldi, G. Maruccio, A. Biasco, V. Arima, R. Cingolani, T. Giorgi, S. Masiero, G. P. Spada, G. Gottarelli, *Nanotechnology* **2002**, *13*, 398; S. D'Amico, G. Maruccio, P. Visconti, E. D'Amone, R. Cingolani, R. Rinaldi, S. Masiero, G. P. Spada, G. Gottarelli, *Microelectron. J.* **2003**, *34*, 961.

[9] T. Giorgi, S. Lena, P. Mariani, M. A. Cremonini, S. Masiero, S. Pieraccini, J. P. Rabe, P. Samorì, G. P. Spada, G. Gottarelli, *J. Am. Chem. Soc.* **2003**, *125*, 14741.

[10] G. Gottarelli, G. P. Spada, P. Mariani, in *Crystallography of Supramolecular Compounds* (Eds.: G. Tsoucaris, J. L. Atwood, J. Lipkowski), Kluwer, Dordrecht, **1996**, p. 307.

[11] V. Luzzati, in *Biological Membranes* (Ed.: D. Chapman), Academic Press, London, **1968**, p. 71.

[12] F. Federiconi, P. Ausili, G. Fragneto, C. Ferrero, P. Mariani, *J. Phys. Chem. B* **2005**, *109*, 11037.

[13] D. Haldar, H. Jiang, J.-M. Léger, I. Huc, *Angew. Chem.* **2006**, *118*, 5609; *Angew. Chem. Int. Ed.* **2006**, *45*, 5483.

[14] D. Neuhaus, M. P. Williamson, *The Nuclear Overhauser Effect in Structural and Conformational Analysis*, VCH, Weinheim, **1989**.

[15] U. Simonis, J. L. Dallas, F. A. Walker, *Inorg. Chem.* **1992**, *31*, 5349; T. K. Shokhireva, M. J. M. Nesset, F. A. Walker, *Inorg. Chim. Acta* **1998**, *272*, 204.

[16] E. Mezzina, P. Mariani, R. Itri, S. Masiero, S. Pieraccini, G. P. Spada, F. Spinozzi, J. T. Davis, G. Gottarelli, *Chem. Eur. J.* **2001**, *7*, 388; A. L. Marlow, E. Mezzina, G. P. Spada, S. Masiero, J. T. Davis, G. Gottarelli, *J. Org. Chem.* **1999**, *64*, 5116; V. Gubala, J. E. Betancourt, J. M. Rivera, *Org. Lett.* **2004**, *6*, 4735.

[17] M. Rappolt, A. Hickel, F. Bringezu, K. Lohner, *Biophys. J.* **2003**, *84*, 3111.

[18] T. S. Lin, J. C. Cheng, K. Ishiguro, A. C. Sartorelli, *J. Med. Chem.* **1985**, *28*, 1481.

[19] R. E. Holmes, R. K. Robins, *J. Am. Chem. Soc.* **1964**, *86*, 1242.

[20] M. Ikehara, T. Maruyama, *Chem. Pharm. Bull.* **1976**, *24*, 565.

Received: August 3, 2006
Revised: November 14, 2006
Published online: January 16, 2007

